Materials Today Communications 51 (2026) 114704

Contents lists available at ScienceDirect

Materials Today Communications

journal homepage: www.elsevier.com/locate/mtcomm

Effect of gamma irradiation on chemico/physical properties and enzymatic hydrolysis of poly(butylene 2,5-furanoate) based films

Bettina Semler [a,*], Felice Quartinello [a], Alessandro Coatti [b], Michelina Soccio [b], Maddalena Negrin [c], Elena Macerata [c,d], Mario Mariani [c,d], Andrea Soldini [e], Ignacio Solaberrieta [f], María Carmen Garrigós [f], Debora Puglia [g], Sara Filippi [h], Patrizia Cinelli [h], Alfonso Jiménez [f], Nadia Lotti [b], Georg M. Guebitz [a]

[a] BOKU-University, Institute of Environmental Biotechnology, Department of Agricultural Sciences, Konrad-Lorenz-Strasse 20, Tulln an der Donau, 3430, Austria
[b] Department of Civil, Chemical, Environmental and Materials Engineering, University of Bologna, Via Terracini 28, Bologna 40131, Italy
[c] Department of Energy, Politecnico di Milano, Piazza L. da Vinci 32, Milano 20133, Italy
[d] National Interuniversity Consortium of Materials Science and Technology, via G. Giusti 9, Firenze 50121, Italy
[e] Gammatom Srl, via XXIV Maggio 14, Guanzate 22070, Italy
[f] Department of Analytical Chemistry, Nutrition & Food Sciences, University of Alicante, San Vicente del Raspeig, ES-03690, Spain
[g] Department of Civil and Environmental Engineering, Università degli Studi di Perugia, Strada di Pentima 4, Terni 05100, Italy
[h] University of Pisa, Department of Civil and Industrial Engineering, Largo Lucio Lazzarino 1, Pisa 56122, Italy

ARTICLE INFO

Keywords:
Poly(butylene 2
5-furanoate)-based films
Gamma ray irradiation
Enzymatic hydrolysis

ABSTRACT

Poly(butylene 2,5-furanoate) (PBF), a bio-based polyester derived from 2,5-furandicarboxylic acid (FDCA), is a promising alternative to conventional polyesters, like polyethylene terephthalate (PET), due to its superior barrier properties, mechanical strength, and recyclability. These characteristics make PBF particularly suitable for specialized purposes, including medical packaging, where structural integrity and sterility, achieved via gamma irradiation, are critical. However, gamma irradiation can induce structural changes like chain scission, branching, and/or cross-linking, which can alter thermal stability, mechanical properties, and biodegradability. In this study, PBF samples were exposed to different doses of gamma rays (10–300 kGy) to investigate the impact of irradiation on structural, thermal and mechanical properties, as well as on enzymatic hydrolysis. At moderate doses (25–50 kGy), chain scission enhanced enzymatic hydrolysis. At higher doses (100–300 kGy), HPLC analysis revealed decreased release of monomers, suggesting presence of not fully hydrolysed dimers and oligomers. GPC analysis, tensile tests and contact angle measurements, indicated structural changes and possible grafting and/or cross-linking in the samples irradiated at the highest doses. TGA, DSC and FT-IR analyses further confirmed chain scission and cross-linking as dose-dependent modifications. This study demonstrates that gamma irradiation can be employed as a pre-treatment to enhance enzymatic degradability of PBF without compromising performance. Moderate irradiation doses were identified as optimal, as they accelerate PBF hydrolysis while preserving the polymers functional properties. Furthermore, such doses are used to sterilize medical devices, including biomedical packaging. These findings contribute to develop sustainable, high-performance polymers for medical and industrial application, advancing circular economy goals and environmental sustainability.

1. Introduction

Polyethylene terephthalate (PET) is a widely used polyester, known for its excellent mechanical properties, thermal stability and high optical transparency. These characteristics make PET a perfect candidate for packaging, textile processing or various other industrial applications [1]. However, when it comes to sustainability and environmental concerns, attention is shifting towards bio-based alternatives that can match or even outperform PET. Among these alternatives, furan-based polyesters derived from 2,5-furandicarboxylic acid (FDCA), such as polyethylene furanoate (PEF), have gained significant attention [2,3]. These materials are not only made from renewable feedstocks but exhibit

* Corresponding author.
E-mail address: bettina.semler@boku.ac.at (B. Semler).

https://doi.org/10.1016/j.mtcomm.2026.114704
Received 27 December 2025; Accepted 19 January 2026
Available online 21 January 2026

superior properties in key parameters. For example, PEF has significantly higher gas barrier properties, with up to ten times higher oxygen and fifteen times higher carbon dioxide barrier characteristics than PET [4–6]. This is due to the unique structure and polarity of the furan ring, which contributes to better preservation of packaged goods, extending its shelf-life, by reducing segment mobility and hindering ring flipping [6,7]. Further, PEF can for example be processed using existing PET manufacturing infrastructure and is compatible with already established recycling streams, which further supports the potential as sustainable, high-performance alternative to PET [8]. In addition to PEF, other FDCA-based polyesters, such as poly(butylene furanoate) (PBF), are emerging as promising candidates for specialized applications. PBF has gained significant interest as a bio-based polymer, also showing a set of very interesting properties for demanding applications. This polyester, like PEF, demonstrates smart barrier and mechanical properties that align with the stringent requirements of, for example, medical packaging, where sterility, mechanical, thermal and chemical resistance are crucial. Regardless of the application, the material must maintain structural integrity and functionality after the sterilization process.

Gamma irradiation, is widely used to eliminate pathogens without compromising packaging functionality [9–11]. However, gamma irradiation is a highly energetic electromagnetic radiation and can thus cause harmful structural changes in polymer. Indeed, such radiations have enough energy to break chemical bonds inducing polymer degradation and thus a decrease of polymer molecular weight. On the other hand, they can also allow polymer chains to cross-link. As a result, the mechanical and thermal properties of the polymer can be altered, leading in most cases to a reduction in polymer performance, such as (film yellowing or discoloration, reduction of thermal stability, detriment of mechanical performances and biodegradation rates) [9]. Depending on radiation dose and specific polymer chemical structure, changes in the molecular weight of a polymer can occur due to gamma radiation, affecting the polymer's physical and mechanical properties, such as tensile strength and elongation at break. Usually, at high gamma radiation doses, crosslinking reactions or formation of larger branched structures prevail, potentially improving its heat resistance, but making polymer stiffer, more rigid, and less flexible, leading to a decrease in the material's elasticity and impact resistance and to an increase of tensile strength and a decrease of stretching [12]. Moreover, at such doses, biodegradation can be negatively affected, due to a 3D rigid network. High radiation dosages could also compromise barrier properties, On the other hand, at lower doses, chain scission reaction prevail, causing a decrement of polymer molecular weight, which in turn causes a reduction of tensile strength and stretching, make the polymer more brittle and less durable. Each polymer reacts differently to ionizing radiation, depending on its chemical structure, thus the right dose rate varies and must be identified on the basis of the polymer. The identification of the right dosage of gamma radiation is therefore crucial for application of furan-based polymers in medical packaging [9,13]. In addition to gamma irradiation, other sterilization methods such as electron-beam treatment can also induce significant changes in the structure and performance of biodegradable polyesters. Previous work has shown that different sterilization techniques can affect thermal stability, mechanical behaviour and degradation characteristics of commercial biodegradable polyesters used in medical devices, highlighting the importance of selecting an appropriate method for each material system [14]. Electron-beam irradiation, in particular, has been reported to alter the molecular architecture and mechanical properties of polymers such as poly(lactic acid) and poly(butylene adipate-co-terephthalate), with the extent and nature of these changes depending strongly on the applied dose [15]. ɣ-irradiation is an efficient physical pretreatment to increase the bacterial biodeterioration and compostability efficiency of both slow-degrading aliphatic and aromatic polyesters and the recalcitrant polyolefins [16,17]. While the enzymatic hydrolysis of PET has been extensively studied in the past two decades, far less is known about the enzymatic decomposition of furan-based polyesters. Yet, enzymatic hydrolysis of PEF has previously been described [18,19]. Initial studies demonstrated that the polyol chain length critically influences hydrolysis efficiency for 2,5-furandicarboxylic acid (FDCA) based-polyesters, with branched diols like 1,2-propanediol enhancing enzyme activity (i.e. Thc_Cut1 cutinase) by 30–40 % when compared to linear analogues, due to reduced crystallinity and improved enzyme accessibility [20]. More recent studies demonstrated promising FDCA recovery strategies, achieving 75 % yield from poly(pentamethylene furanoate)/PLA blends through selective enzymatic depolymerization, though this efficiency dropped to 50 % in multiblock copolymers due to morphological constraints [21]. For industrial scalability, enzyme engineering approaches like directed evolution are now being employed to develop PEFases with enhanced thermal stability (targeting >70 °C operational ranges) and increased activity against crystalline regions [22]. Crucially, enzymatic susceptibility correlates strongly with environmental biodegradation rates, serving as a predictive metric that reduces testing timelines from months to days while enabling targeted polymer design. This correlation has been previously described in studies on the enzymatic hydrolysis and biodegradation of coated cellulose sheets as well as ionic phthalic acid-based polyesters, confirming the predictive value of enzymatic degradation assays for environmental performance [20,23–25]. This dual functionality positions enzymatic processing as a cornerstone technology - simultaneously advancing circular economy goals through closed-loop monomer recovery and accelerating the development of next-generation bio-based polymers with optimized end-of-life profiles [21,22]. In this study, we investigate the effect of gamma ray doses on thermal and mechanical properties and on enzymatic hydrolysis of PBF. In particular, we aim to evaluate how structural changes induced by irradiation influence enzyme accessibility and depolymerization efficiency.

2. Materials and methods

2.1. Chemicals and substrates

Di-Potassium hydrogen phosphate (K_2HPO_4) for buffer preparation was purchased from Roth (Karlsruhe, Germany). Other chemicals and pure monomers (2,5-furandicarboxylic acid, 1,4-butanediol, succinic acid, 1,5-pentanediol) for instrument calibration and purity comparison were purchased from Sigma-Aldrich (Vienna, Austria). The commercially available cutinase from *Humicola insolens* (hereby abbreviated as HiC) was from Novonesis (Copenhagen, Denmark).

2.2. Synthesis of Poly(butylene furanoate) (PBF)

Poly(butylene 2,5-furanoate) (PBF) was synthesized through a well-established two-step bulk polycondensation process [26]. The reaction was carried out in a 250 mL thermostatted glass reactor equipped with mechanical stirring. The reactor was charged with 2,5-furandicarboxylic acid dimethyl ester and 1,4-butanediol (1,4-BD) at a molar ratio of 1:1.5, along with tetrabutyl titanate (TBT) and titanium isopropoxide (TIP) as catalysts, each at a concentration of 200 ppm. The first stage of the reaction, namely transesterification, was conducted under an inert nitrogen atmosphere at 190 °C with continuous stirring (50 rpm). Methanol, released as a by-product, was continuously removed by distillation and collected in a downstream glass trap. The conclusion of transesterification was determined by the collection of 90 % of the theoretical amount of methanol, which was achieved after 90 min. In the subsequent polycondensation step, the reaction mixture was gradually heated to 220 °C while the system pressure was progressively reduced to 0.05 mbar. This stage proceeded for 3.5 h until a constant torque value was reached, indicating the completion of polymerization. The resulting polymer was then discharged from the reactor and stored at room temperature for further characterization.

2.3. Molecular characterization

^{1}H and $^{1\ 3}$C NMR spectroscopy were employed to determine the chemical structure of the as-synthesized PBF. Therefore, samples were prepared by dissolving 10 mg mL^{-1} and 30 mg mL^{-1} for ^{1}H and $^{1\ 3}$C NMR, respectively, in deuterated chloroform, with tetramethylsilane (TMS, 0.03 vol%) as an internal reference. An aliquot of trifluoroacetic acid (TFA) were added to facilitate polymer dissolution. NMR measurements were performed using a Varian XL-400 spectrometer (Palo Alto, CA, USA) at 25 °C. ^{1}H NMR spectra were acquired with a relaxation delay of 0 s, an acquisition time of 1 s, and up to 100 scans. $^{1\ 3}$C NMR spectra were recorded with a relaxation delay of 1 s, an acquisition time of 1 s, and up to 700 scans (For additional information on the NMR spectra, refer to SI Figure S1 and S2). Gel permeation chromatography (GPC) was used to determine the molecular weight of neat PBF both before and after gamma irradiation. Analysis was performed on a Jasco (Cremella, Italy) GPC system equipped with a PU-2089 Plus pump, a UV-4075 detector ($\lambda = 254$ nm), a Peltier column oven (CO-4060), and an AS-2055 Plus autosampler. Measurements were conducted at 30 °C using a Phenogel column (5 μm particle size, 10^4 Å pore size, 300 × 7.8 mm), with a molecular weight operating range of 5000–500,000 Da, and a Phenogel 5 μm Linear/Mixed guard column (50 × 7.8 mm, Phenomenex). The injection volume was 5.0 μL, and the mobile phase consisted of a chloroform/hexafluoroisopropanol (98/2 % v/v) solution. Samples were dissolved at room temperature in the eluent at a concentration of approximately 5 mg mL^{-1}. The solvent flow rate was maintained at 1.0 mL min^{-1}. Prior to injection, samples were filtered through a 0.45 μm PTFE filter. The instrument was calibrated using monodisperse polystyrene standards analyzed under identical conditions to establish the correlation between retention times and molecular weights. Gravimetric tests were performed to evaluate the dose dependence of the gel fraction in PBF irradiated samples. About 300 mg, accurately weighted, of the irradiated PBF sample were dissolved in 25 mL of CHL/HFIP 98/2 vol/vol. The solution was filtered, under vacuum, using a pre-weighted sintered glass filter to recover the undissolved gel fraction eventually present. The filter was dried under vacuum at 50°C to determine the weight of the insoluble fraction.

2.4. Film preparation

Before processing, PBF granules were dried at 40 °C overnight to reduce the moisture content and to avoid hydrolysis phenomena during extrusion. Granules were then processed by a co-rotating twin screw microextruder (Xplore 5&15cc Micro Compounder, Sittard, The Netherlands). Films with a width of approximately 60 mm and nominal thickness of 50 μm were obtained by coupling the extruder with a 65 mm Xplore Film Device and using temperature-controlled cast film die. The temperature profile was set at 220–230 - 240 °C in the three heating zones of the extruder, mixing for 3 min at a screw speed of 60 rpm. The temperature was set at 210 °C, film line at a drawing speed of 200 mm min^{-1} of the draw-off roller and a winding torque of 60 N·mm for the take-up roller.

2.5. Irradiation of polymers

Gamma irradiation of the polyester samples was carried out at Gammatom srl (Guanzate (CO), Italy) utilizing a commercial ^{60}Co gamma source as part of their routine industrial processing cycles. The irradiations were performed in air at room temperature with a nominal dose rate, certified by the provider for the specific batch configuration, of approximately 2.5 h^{-1}. A series of target absorbed doses was applied: 10, 25, 50, 75, 100, 200, and 300 kGy. Prior to irradiation, the polyester samples were carefully arranged within their primary packaging, sealed padded paper envelopes, to prevent overlapping. These packages were then delivered to Gammatom srl, who integrated them into a larger industrial batch loaded onto standard carriers (pallets). The positioning and overall loading density of the batch were managed by the irradiation provider according to their established protocols, designed to ensure accurate dosimetry within the industrial gamma facility. Routine dose mapping, conducted by Gammatom srl for the specific loading configuration of each cycle, identified the positions receiving the minimum (cold spot) and maximum (hot spot) absorbed doses within the batch volume. To evaluate the dose range experienced at the sterilization target level (25 kGy), sample packages were positioned by the provider at both the minimum and maximum dose locations identified in the map. For all higher target doses (from 50 kGy to 300 kGy), the sample packages were consistently placed by Gammatom srl at the predetermined minimum dose (cold spot) position relevant to that batch configuration. Therefore, the reported nominal target doses correspond to the minimum absorbed dose certified for that position within the industrial cycle.

2.6. Enzyme characterization: protein concentration and activity assay

The enzyme concentration in the stock solution was determined via the Bradford assay. Therefore, 10 μL of the diluted sample and water as blank was placed in triplicate in a transparent 96-well Greiner plate. Additionally, 200 μL of the 1:5 diluted Bradford reagent was followed by a 5-min room-temperature incubation while shaking. A Tecan plate reader was then used to measure the absorbance at 595 nm and the concentration was subsequently calculated referring to bovine serum albumin protein as standard. To determine esterase activity, *para*-nitrophenylbutyrate (*p*-NPB) was used as a substrate. Precisely, 20 μL of the enzyme (prediluted in ultrapure water to 1:100 and 1:1000) were placed in triplicate in a transparent 96-well Greiner plate. Then, 200 μL of the substrate (diluted in DMSO and buffer of incubation) was added to both the enzyme dilutions and the blank (buffer). The absorbance at 405 nm was measured for 10 min at 25 °C every 18 s. The activity was expressed in units mL^{-1}.

2.7. Enzymatic treatment of PBF films

The polymers were cut in circles with a diameter of 7 mm (average weight 4.0 ± 0.7 mg) and washed in three subsequent steps to remove surface impurities: Triton X-100, Na_2CO_3, and a final rinsing with ultrapure water. The enzyme solutions were prepared in 0.1 M KPO buffer pH 8 (K_2HPO_4/KH_2PO_4) to a final concentration of 5 μM. The films were incubated in Eppendorf tubes with 2 mL of enzyme dilution at 70 °C under agitation (150 rpm). The reaction was monitored throughout the incubation course, collecting samples after 0, 24, 48 and 72 h to follow the decomposition pattern. The reaction was stopped at different time points by cooling down to 4 °C, a temperature at which the enzyme activity is negligible. The enzyme was then removed from the hydrolysate and Methanol and Carrez precipitation were performed with the supernatant. At the same time, a set of 3 blanks per each film type was incubated with buffer only as controls. For each time point experiments were performed in triplicate.

2.8. Weight loss and surface characterization of the polymers using SEM

For samples with remaining polymer after hydrolysis, the residual weight was recorded and compared to the initial weight of the sample after the washing step. This weight difference served as a primary evaluation of the efficacy of enzymatic treatment. Scanning electron microscopy (SEM) images were acquired using a Hitachi 3030 TM (Metrohm INULA GmbH, Austria) at a set of increasing magnifications (100X, 1000X and 2500X). Images were acquired after applying a 2 nm platinum coating.

2.9. Quantification of soluble reaction products via HPLC

The hydrolysates after each time point were quantified for the

released monomers via high-performance liquid chromatography (HPLC) instruments (Agilent Technologies, 1260 Infinity, California, USA) equipped with reversed-phase column C18 for aliphatic monomer like 1,4-butanediol. Samples for HPLC analysis were cleaned from proteins through Carrez clarification based on potassium hexacyanoferrate (II) trihydrate and zinc sulfate heptahydrate reagents. The two reagents were added sequentially to the hydrolysate. Thereafter, a centrifugation step was performed (30 min, 14000 rpm, 4 °C) before filtering the clear supernatant into an HPLC vial. HPLC in use was coupled with a refractive index detector (Transgenomic IC SEPION-300) and run in 0.01 N H_2SO_4 with a flow rate of 0.325 mL min^{-1}, 45 °C. For the aromatic compound FDCA, a UV detector was used; the gradient was based on methanol and 0.1 % formic acid at a flow rate of 0.325 mL min^{-1}, while the injected volume was 10 μL. The equilibration of the column to the initial gradient was carried out after each run for a total of 20-min run per sample. The preparation of samples for the HPLC analysis included a methanol-based precipitation protocol aiming at the removal of the enzyme from the solution. In short, samples were diluted in ice-cold methanol (1:1 ratio) and 10 μL 6 N HCl was added. Centrifugation for 30 min (14000 rpm, 4 °C) was performed and the isolated supernatant was subsequently filtered (0.2 μM polyamide filters) into HPLC vials. The concentration of the hydrolysis products was calculated based on calibration curves for the two monomer standards, FDCA (0.001–0.5 mM) and 1,4-butanediol (0.1–20 mM), prepared and measured in the same manner as the samples (SI: Figure S3 and S4).

2.10. Water contact angle measurements

Static water contact angle (WCA) measurements were carried out at room temperature on neat and gamma-irradiated PBF samples using a KRUSS DSA30 instrument. The side profiles of the deionized water drop (4 μL) were recorded and analyzed 30 s after drop deposition using drop shape analysis software. Tests were performed by depositing at least five drops on both sides of the material strip, and water contact angles (WCA) were reported as the average value ± standard deviation. Each drop was deposited on the films by placing it in contact with the polymeric surface using the syringe needle.

2.11. Fourier transform infrared spectroscopy (FTIR)

The chemical structure of neat and gamma-irradiated PBF samples was analyzed using FTIR. Spectra were obtained using Jasco FTIR 4700 IRT-5200 (Easton, MD, USA) and PerkinElmer (Massachusetts, USA) instruments in attenuated total reflectance (ATR) mode. Analyses were performed in the 4000–650 cm^{-1} range with a spectral resolution of 2–4 cm^{-1} and 40 scans per measurement as indicated below.

2.12. Thermogravimetric analysis (TGA)

Thermal stability of pristine and gamma-irradiated PBF samples was evaluated by TGA using a Mettler Toledo TGA/SDTA 851e equipment (Schwarzenbach, Switzerland). Approximately 5 mg of each sample were placed on alumina pans and heated from room temperature to 800 °C at a heating rate of 10 °C min^{-1} under nitrogen atmosphere (50 mL min^{-1}). The onset temperature at 1 % of heating loss ($T_{1\ \%}$), the temperature of maximum degradation rate (T_{max}) and the remaining residue at 800 °C were determined to characterize the thermal decomposition process.

2.13. Differential scanning calorimetry (DSC)

Thermal transitions of pristine and gamma-irradiated PBF samples were evaluated using a TA instruments Q2000 calorimeter (New Castle, DE, USA). Approximately 5 mg of each sample were placed into closed aluminum pans and subjected to analysis under nitrogen atmosphere (50 mL min^{-1}). The thermal program consisted of a first heating cycle from room temperature to 250 °C, followed by cooling to −90 °C, and a further second heating to 250 °C. All cycles were performed at 10 °C min^{-1} and were followed by a 3-minute holding stage at their endpoint temperatures. An empty aluminum pan was used as reference. The glass transition temperature (T_g) was determined using the midpoint approach. Crystallization (T_c) and melting temperatures (T_m) were obtained from the maximum of the exothermic and endothermic peaks, respectively. Enthalpies of fusion (ΔH_m) and crystallization (ΔH_c) were calculated from the integrated areas under the corresponding melting and crystallization peaks.

2.14. Mechanical characterization

The mechanical characterization of pristine and irradiated PBF samples was performed using an Instron 5966 dynamometer (Norwood, MA, USA) equipped with rubber grips and a 10 kN load cell coupled to a transducer and controlled by a computer. Tests were carried out at room temperature and 50 % relative humidity, with a gauge length of 20 mm and a strain rate of 10 mm min^{-1} until failure. The load-displacement data were converted into stress-strain curves, from which the tensile elastic modulus (E) was determined from the initial linear slope. Additionally, elongation at break (ε_b) and stress at break (σ_b) were measured. At least three specimens per sample were tested, and results were reported as mean values ± standard deviation.

3. Results and discussion

3.1. Molecular characterization of irradiated PBF-based films

PBF-based films were subjected to gamma-ray irradiation in air atmosphere using different doses. Among these, a dose routinely employed for sterilization of medical packaging (25 kGy). Results on the number-average molecular weight (M_n) of pristine and irradiated PBF samples are reported in Table 1, along with the dispersity index (Đ) and water contact angle values. Up to a dose of 100 kGy, the PBF molecular weight decreased with increasing irradiation dose (-19.2 % at 100 kGy), while the dispersity remained unchanged. This trend is visually depicted in Fig. 1, which shows the shift in molecular weight distribution curves for PBF sample exposed to different irradiation doses. The increment of irradiation dose leads indeed to a progressive leftward shift in the molecular weight distribution, i.e. the higher the dose the lower the molecular weight. (For additional quantitative data on average molecular weight values, refer to SI Table S1.).

This suggests that chain scission reactions take place predominantly, leading to the cleavage of long polymer chains into smaller segments, while maintaining an approximately constant M_w/M_n ratio. A notable decrease in the molecular weight was observed in the samples irradiated at 200 and 300 kGy, with reductions of 27.7 % and 54.2 %, respectively. At the same time, a decrease in the dispersity index is also observed. It should be noted that the sample irradiated at the highest dose is no longer completely soluble in chloroform, thus the GPC data reported in

Table 1
Number-average molecular weights (M_n), dispersity (Đ), and water contact angle results as a function of irradiation dose.

	GPC		WCA
PBF sample	**M_n (g/mol)**	**Đ**	**(°)**
Neat	52573	2.01	79 ± 3
10 kGy cold spot	53375	2.00	81 ± 2
25 kGy cold spot	48978	2.02	79 ± 3
25 kGy hot spot	48650	2.03	79 ± 2
50 kGy cold spot	45853	2.03	78 ± 3
75 kGy cold spot	44150	2.00	81 ± 2
100 kGy cold spot	42490	1.99	82 ± 3
200 kGy cold spot	38009	1.85	75 ± 2
300 kGy cold spot	24061	1.44	73 ± 2

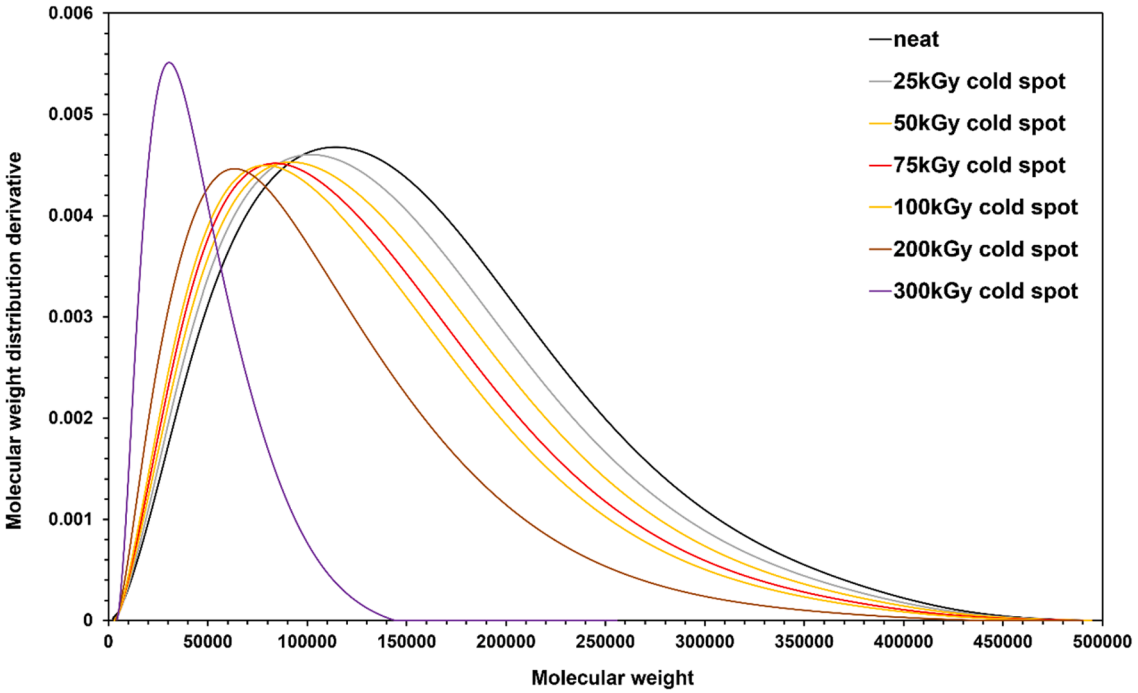

Fig. 1. Trend of the molecular weight distributions of pristine and irradiated PBF samples.

Table 1 refer only to the soluble fraction of the sample. The reduced solubility in chloroform is a clear indication that at least partial crosslinking occurred. This also explains the decrease in dispersity, as only the molecular weight of non-crosslinked polymer fraction could be dissolved and measured.

In the gravimetric tests evaluating the dose dependence of gel fraction in PBF irradiated samples, all materials irradiated up to 50 kGy (specifically 0, 10, 25, and 50 kGy) were completely soluble and exhibited no detectable gel fraction. At 100 kGy, a gel fraction of 11.2 wt% was observed, indicating the onset of crosslinking. When the irradiation dose was increased to 200 kGy and 300 kGy, the samples became extremely difficult to filter and appeared to be almost fully crosslinked, with gel fractions approaching 100 %. As to the film wettability, WCA values remain constant for doses up to 100 kGy, and then decrease at the two highest doses (200 and 300 kGy). The trend is in agreement with the molecular weight data trend. Chain breaking reactions, in fact, determine an increment in the terminal functional groups (mainly hydroxyl and carboxylic ones) with a consequent increase in the hydrophilic nature of the film. The ATR-FTIR spectra of pristine and gamma-irradiated PBF films are presented in Fig. 2. The pristine PBF spectrum is in close agreement with previous reports [27–29]. The observed signals could be assigned to different molecular groups as follows. The sharp absorption bands characteristic of ester groups C═O, (C-O-C) asymmetric and (C-O-C) symmetric stretching vibrations were observed at 1714, 1267 and 1129 cm^{-1}, respectively. Several bands corresponding to the 2,5-furan heterocycle vibrations were also present in FTIR spectra. The stretching vibration of =C-O-C= was observed at 1220 cm^{-1}. Moreover, the stretching vibrations corresponding to aromatic C═C bonds were located at 1508 and 1574 cm^{-1}. Stretching vibrations of =C-H bonds were observed at 3125 and 3169 cm^{-1}. Furthermore, several signals corresponding to out-of-plane deformation of the furan ring were observed in the fingerprint region at 763, 822 and 965 cm^{-1}. Finally, bands corresponding to both the symmetrical and asymmetrical stretching modes of $–CH_2–$ groups corresponding to the butylene glycol subunit were observed at 2853–2960 cm^{-1}, respectively. As can be observed from Fig. 2, all main characteristic PBF signals were also present in the spectrum of gamma-irradiated samples and no significant shifts were

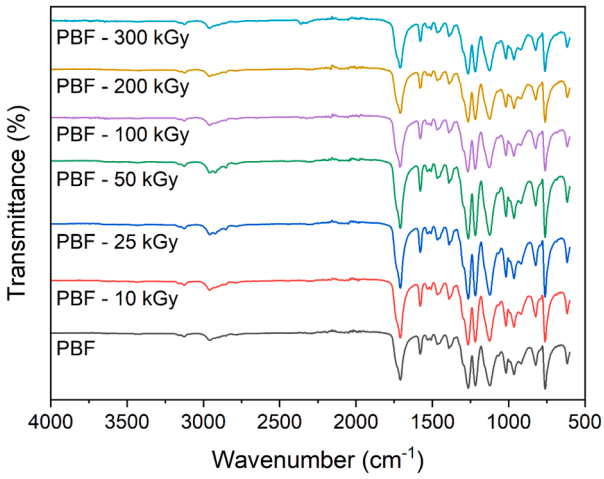

Fig. 2. FTIR spectra of neat and gamma-irradiated PBF samples (spectral resolution 4 cm-1 and averaging 32 scans per measurement).

observed. In fact, the position of the characteristic bands remained constant independently of the irradiation dose. The only slight difference could be noted around 2850 cm^{-1}, in particular for samples irradiated at doses higher than 25 and 50 kGy, which could be related to some degree of cross-linking. These signals are less prominent at higher irradiation doses, suggesting that further crosslinking is minimal beyond this point.

3.2. *Thermal characterization of irradiated PBF-based films*

3.2.1. *Thermal stability of gamma-irradiated PBFs*

The thermal stability of neat and gamma-irradiated PBF polymers was evaluated by using TGA under nitrogen atmosphere. The TGA curves are shown in Fig. 3. Characteristic parameters of the thermal degradation process are summarized in Table 2. All samples exhibited a nearly negligible initial weight loss stage observed around 100 °C, which

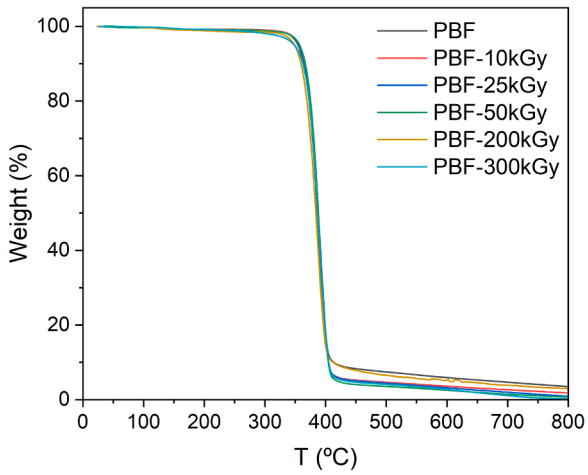

Fig. 3. TGA thermogram of neat and gamma-irradiated PBF samples.

Table 2
Thermal decomposition parameters of gamma-irradiated PBF samples (n = 2).

PBF-Sample	$T_{1\ \%}$ (°C)	T_{max} (°C)	$RES_{800°C}$ (%)
Neat	332.1 ± 3.6	387.2 ± 2.7	4.7 ± 1.6
10 kGy	336.6 ± 0.5	390.4 ± 0.1	1.7 ± 0.2
25 kGy	336.8 ± 0.2	391.1 ± 1.0	1.3 ± 0.4
50 kGy	333.8 ± 0.9	389.8 ± 0.8	0.9 ± 0.2
200 kGy	317.3 ± 15.8	385.0 ± 2.3	3.8 ± 1.3
300 kGy	282.0 ± 1.3	388.7 ± 0.9	0.30 ± 0.04

was associated to moisture and volatiles desorption. This step was followed by a single-step degradation process, which extended up to approximately 400 °C. It has been reported that polymeric materials are sensitive to radiation. As a result, their properties may undergo significant changes after exposure, depending on the type of material and the radiation dose. During the gamma irradiation, as discussed above, two competing mechanisms occur simultaneously: on the one hand, cross-linking can lead to molecular rearrangement and the formation of new bonds; on the other hand, chain scission promotes the degradation of the polymer chains [10,30–32]. The dominant mechanism is influenced by both the polymer characteristics and morphology and the absorbed radiation dose. For the pristine PBF, the onset decomposition temperature was observed at approximately 334.7 °C. This temperature slightly increased with irradiation up to a dose of 50 kGy. However, at higher doses the decomposition started at progressively lower temperatures, with a notably lower onset observed at 300 kGy. This suggests that the polymer structure might suffer some deterioration with high doses of gamma-irradiation. Therefore, at doses above 50 kGy, chain scission may become the dominant process over cross-linking. In contrast, no significant differences were found regarding the temperature of maximum degradation rate, being approximately 390 °C across all samples. Finally, the amount of char residue remaining at the end of the experiment gradually decreased from 3.55 % corresponding to the pristine sample to 0.26 % for the 300 kGy irradiated sample. This result contrasts with the expectation of crosslinking as the predominant mechanism for high doses, but differences are not so significant to correlate chart formation with irradiation doses.

3.2.2. Thermal behavior of gamma-irradiated PBFs

Table 3 summarizes the thermal parameters T_g, T_m and T_c representing the glass transition, melting and crystallization temperatures, respectively, while ΔH_m and ΔH_c correspond to the melting and crystallization enthalpies. All samples exhibited a very subtle glass transition temperature around 40 °C with no significant variation with irradiation doses. This thermal transition was followed by a melting event during the second heating cycle as well as a crystallization transition when cooling from the melt. As detailed in Table 3, the thermal behavior of both neat and gamma-irradiated PBFs showed dependence on the irradiation dose following a trend consistent with the findings from TGA results (For additional DSC curves, refer to SI Figure S5.). A slight increase in the melting temperature was observed up to intermediate irradiation, followed by a decrease at higher doses. Analogously, a similar trend was observed during the cooling curve in the crystallization temperature. This decrease in both, the melting and crystallization temperatures, with the increasing radiation dose has been reported by other authors. Gamma irradiation promotes competing mechanisms such as cross-linking, chain scission and oxidative degradation, all of them can affect the crystalline structure of the materials. Extended or intensive exposure to gamma irradiation might lead to progressive chain scission, which results in shorter molecular chains and changes in temperature of the thermal transitions. Therefore, a decrease in T_m reflects the deterioration of the polymer crystalline regions at high doses. These findings are consistent with other studies conducted in other polymer materials. For instance, Vasile *et al.* [33] studied the effect of gamma irradiation on PLA-based blends and composites and observed a decrease of the melting temperature with increasing gamma irradiation dose. Moreover, Suárez *et al.* [34] observed a similar decline in melting temperature of gamma-irradiated LDPE, while Kattan [35] reported similar behavior in PET films subjected to gamma irradiation and Sirin *et al.* [36] on polypropylene and polyethylene blends. On the other hand, no clear trend was observed in the enthalpy values associated with either the melting or crystallization transitions as a function of the gamma irradiation doses.

Table 3
Thermal parameters for neat and gamma-irradiated PBF.

PBF-Sample	T_g (°C)	T_m (°C)	ΔH_m (J g^{-1})	T_c (°C)	ΔH_c (J g^{-1})
Neat	40.2 ± 1.7	167.8 ± 0.2	36.1 ± 2.0	130.2 ± 0.3	49.4 ± 2.0
10 kGy	40.9 ± 0.1	168.5 ± 0.1	41.0 ± 0.2	130.8 ± 0.1	54.3 ± 0.6
25 kGy	39.7 ± 0.7	168.4 ± 0.1	38.7 ± 0.7	130.6 ± 0.4	50.9 ± 0.7
50 kGy	38.7 ± 1.5	168.2 ± 0.5	38.0 ± 0.1	131.9 ± 1.3	50.7 ± 0.1
100 kGy	37.5 ± 0.1	167.9 ± 0.1	38.6 ± 0.1	132.0 ± 0.1	50.8 ± 1.0
200 kGy	42.8 ± 0.2	165.7 ± 0.1	37.9 ± 0.2	128.1 ± 0.1	50.5 ± 0.8
300 kGy	41.0 ± 1.0	164.5 ± 0.1	37.9 ± 1.3	126.2 ± 0.1	50.9 ± 1.6

3.3. Mechanical response of irradiated PBF-based films

The mechanical response of irradiated PBF samples changed according to the irradiation dose, the effect being higher as the dose is increased (Table 4). Indeed, at low and moderate doses (up to 100 kGy)

Table 4
Tensile properties of PBF samples after exposure to different irradiation doses, showing Young's modulus (E), tensile strength (σ_b), and elongation at break (ε_b).

PBF sample	Tensile test E(MPa)	σ_b (MPa)	ε_b (%)
Neat	1503 ± 104	55 ± 17	414 ± 80
10 kGy cold spot	1514 ± 165	61 ± 8	461 ± 57
25 kGy cold spot	1671 ± 68	57 ± 3	456 ± 31
25 kGy hot spot	1440 ± 50	58 ± 2	369 ± 10
50 kGy cold spot	1573 ± 155	58 ± 5	432 ± 40
75 kGy cold spot	1449 ± 67	58 ± 9	395 ± 23
100 kGy cold spot	1447 ± 84	62 ± 8	420 ± 48
200 kGy cold spot	2200 ± 74	43 ± 9	190 ± 146
300 kGy cold spot	2676 ± 53	67 ± 1	3.03 ± 0.08

the elastic modulus, stress at break and strain at break remained relatively stable, with variations falling within the standard deviation. This suggests that the polymer maintains its original ductility and mechanical integrity, as also observed in similar polyesters subjected to moderate irradiation [37,38]. The elastic modulus remained around 1500 MPa, and the strain at break kept above 400 %, indicating the preservation of polymer ductility and flexibility. With a further increase in the absorbed dose (above 100 kGy), the prevalence of cross-linking over chain scission occurs. At 200 kGy, the elastic modulus increased sharply to 2200 ± 74 MPa, while the strain at break dropped dramatically to 190 ± 146 %. These changes are attributed to an increased degree of cross-linking within the polymer network, which restricts chain mobility and results in a stiffer, more brittle material. The observed properties of the highly irradiated PBF samples exhibited two opposing effects. On one hand, the increased material degradation, resulting in a higher concentration of terminal functional groups, would explain the enhancement in surface wettability. On the other hand, the increase in elastic modulus coupled with the substantial reduction in elongation at break indicates a pronounced cross-linking of the material. These two phenomena seem to coexist at high gamma irradiation doses, consistent with findings in literature on radiation induced cross-linking in polymers [39]. The decrease in molecular weight and dispersity at higher doses, as observed in the GPC data, supports this interpretation. Only the non-crosslinked fraction remains soluble and measurable [40]. The effects of irradiation at 25 kGy, which is considered a typical sterilization dose, should be carefully considered. Both, the hot spot and cold spot regions of the PBF were analyzed at this dose. As noted above, despite a slight reduction in molecular weight, the material maintained its original properties. Overall, while low to moderate irradiation doses preserve the mechanical performance of PBF, high doses induce significant cross-linking, leading to increased stiffness but a dramatic loss of ductility and toughness [41,42] (Corresponding stress-strain curves, refer to Figure S6).

3.4. Enzymatic degradation of irradiated PBF-based films

The enzyme investigated for hydrolysis of PBF, namely a cutinase from *Humicola insolens* (HiC), had a total protein concentration of 0.9 ± 0.2 mg mL^{-1} and an activity of 0.58 ± 0.02 mg mg^{-1} on p-NPB. The optimal temperature and buffer conditions were adopted according to previous work [43]. The reason for choosing HiC is due to its wide use for the hydrolysis of a wide range of polyesters, including such containing furan rings [19]. From the PBF films irradiated at 25 kGy and 50 kGy, nearly identical amounts of monomers were released after 72 h of enzymatic hydrolysis. Interestingly, the overall amounts were much higher than those seen for the non-irradiated sample and for those irradiated at higher doses (Fig. 4). In contrast, the 100 kGy treated PBF film showed slightly lower monomer release. From the 200 kGy and

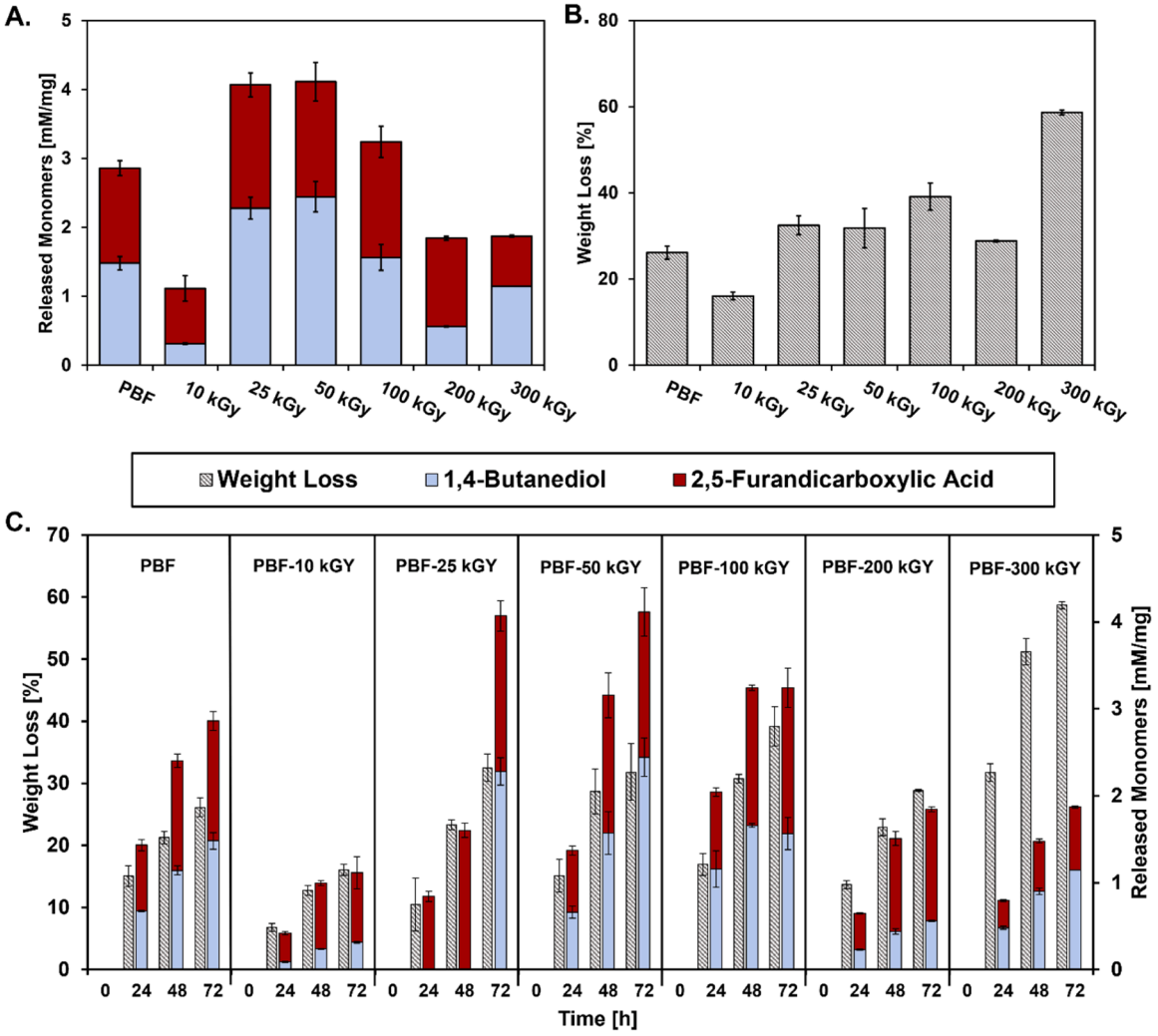

Fig. 4. Effect of gamma irradiation on enzymatic degradation of PBF. **A.** Total released monomers [mM mg^{-1}] after 72 h of enzymatic hydrolysis (blue: 1,4-butanediol; red: 2,5-furandicarboxylic Acid). **B.** Corresponding weight loss [%] (hatched bars). **C.** Time-course analysis of weight loss and monomer release over 0, 24, 48 and 72 h for each irradiated PBF sample.

300 kGy treated PBF films, similar total amounts of monomers were released, but their distribution was different. The 200 kGy PBF released more 1,4-butanediol, whereas the 300 kGy PBF film showed higher FDCA levels at the end of hydrolysis. The lowest monomer release was observed for PBF film treated with 10 gamma rays (Fig. 4A) which showed a slight increase in molecular weight and WCA when compared to the control. In terms of weight loss, the 10 kGy irradiated PBF film also exhibited the lowest reduction after 72 h of reaction. The 25 kGy and 50 kGy PBF samples again showed similar weight loss levels. However, the highest weight loss, more than 60 %, was observed in the PBF treated with 300 gamma irradiation (the highest investigated dose), followed by the 100 kGy, 200 kGy, and pristine PBF samples (Fig. 4B). In Fig. 4C, the degradation patterns over the time of 0, 24, 48 and 72 h are shown. The weight loss and monomer release are increasing over time and the distribution between the monomers released is similar. However, for the PBF treated with 25 kGy dosage of gamma irradiation, during the first 48 h only 1,4-butanediol was released, while after 72 h FDCA could be also quantified. Further, only the 300 kGy treated PBF sample showed higher weight loss as would be expected from the monomers released (Fig. 4C). This suggests that the low molecular weight polymer fractions generated by the 300 kGy treatment (as proved by the GPC decrement of molecular weight of soluble PBF fraction) is promptly attacked by the enzyme. The differences in monomer release and weight loss across the different gamma-irradiated PBF films can be explained by structural and chemical modifications occurring during the irradiation process, as discussed in detail above. 25–50 kGy is in the range of moderate irradiation where it is likely that predominantly chain scission takes place in the polymeric structure. On the other hand, higher dosages (100–300 kGy) may lead to chain scission as well as to crosslinking, which leads to coexistence in the film of oligomers that can be efficiently attacked by the enzyme and of recalcitrant cross-linked portions [24]. For the 300 kGy treated film, a higher weight loss than expected from the released monomer was seen suggesting enhanced low molecular weight water-soluble oligomers (escaping HPLC quantification) due to polymer chain scission at this high radiation dose. These results also align with observations e.g. reported for polyurethane-polyester copolymers, along with HiCs surface erosion mechanism generating enough cracks and reducing molecular weight without complete monomerization. On the other hand, the delayed FDCA release seen for the 25 kGy treated films indicates that HiC targets first accessible ester bonds throughout irradiated amorphous regions before hydrolyzing far more stable crystalline domains [44,45]. Irradiation-prompted structural changes of PBF films probably echo thermal or mechanical pre-treatment effects noted for PET hydrolysis. In PET hydrolysis, the modified polymer morphology was reported to improve enzymatic hydrolysis [44,46]. The relatively and comparably lower efficiency seen in this study for 10 kGy treated PBF reflects insufficient irradiation to fully disrupt crystallinity, thereby limiting enzymatic hydrolysis to surface layers.

The SEM images (Fig. 5) illustrate the surface morphology in a 2500x resolution of PBF films before and after enzymatic hydrolysis for 72 h, giving visual insight into the impact of gamma irradiation on polymer degradation. At 0 h, all samples showed smooth surfaces, with slight roughness in the gamma irradiated films, especially at higher dosages (100–300 kGy), which could be already an indicator for structural modifications. After 72 h of enzymatic hydrolysis, there was a significant change in the surface morphology. The non-irradiated PBF sample showed minimal surface erosion, which is consistent with a low amount of monomers released and low weight loss due to structural changes, which can limit the accessibility of the enzyme on the structure. This is also similar to the sample irradiated with 10 kGy. The SEM microscopy shows minor degradation suggesting that low dosages did not disrupt the structure efficiently enough to improve enzymatic hydrolysis. In contrast, the samples treated at 25 and 50 kGy show more surface degradation including cavities and cracks, which also correlates with their highest weight loss and monomer release. This confirms that moderate gamma irradiation dosages enhance accessibility for the enzyme by increasing amorphous regions. Consequently, this could be an ideal radiation dose to both, ensure sterilization of medical packaging films and concomitantly enhance biodegradation. The 100 kGy and 200 kGy samples showed slightly less intense surface modification when compared to the 25–50 kGy samples, because of crosslinked polymer fraction. Finally, the 300 kGy treated PBF film also showed extensive surface erosion reflecting the significant weight loss.

In this case, the crosslinked portion coexists with soluble low molecular weight polymer chains that are efficiently degraded by enzyme. The FT-IR spectra provide insights into the change of the chemical structure after enzymatic hydrolysis of the PBF films (Fig. 6).

After 72 h of enzymatic hydrolysis (Fig. 6), changes were observed in

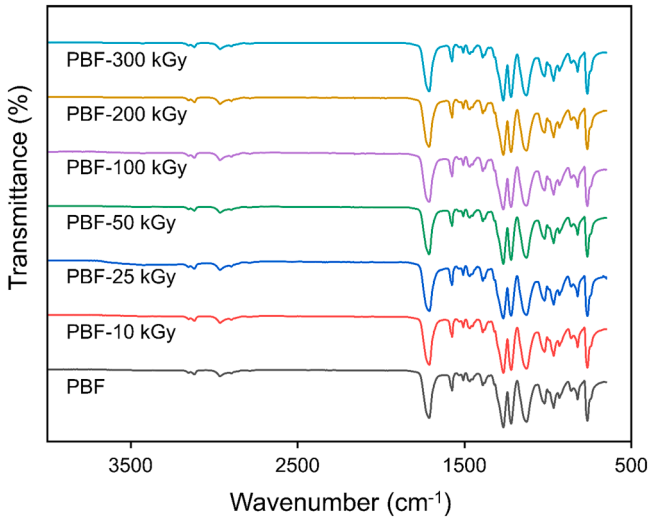

Fig. 6. FT-IR spectra of PBF and irradiated PBF after 72 h of enzymatic hydrolysis. Spectra were recorded from 650 to 4000 cm^{-1} for 40 scans (resolution 2 cm^{-1}).

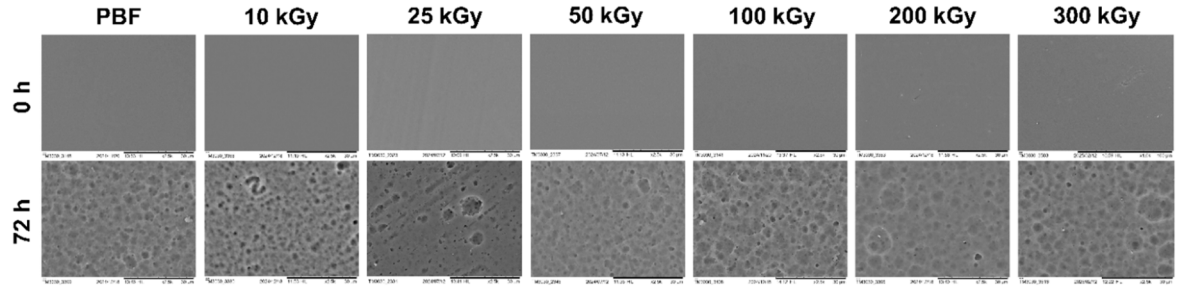

Fig. 5. SEM imaging of PBF film enzymatically hydrolyzed for 3 days (72 h; bottom row) and the respective control (0 h; buffer only, upper row) at 2500x magnification.

all the spectra compared to Fig. 2. The intensity of the ester-bond peaks (~ 1700 cm^{-1}) is altering in each sample, especially within the neat PBF, 10, 200 and 300 kGy, indicating the enzymatic hydrolysis. The most pronounced reduction can be seen in the 25–50 kGy polymers. However, there were also residual peaks at lower wavenumbers indicating the presence of oligomers or dimers resulting from incomplete depolymerization. The untreated PBF and 10 kGy samples only showed minimal spectral changes, consistent with their limited enzymatic decomposition. These results confirm that gamma irradiation enhances enzymatic hydrolysis efficiency by modifying polymer structure, with moderate doses (25–50 kGy) providing optimal conditions for ester bond cleavage.

4. Conclusion

This study provides a consistent insight into the structural and functional transformations of poly(butylene furanoate) films subjected to gamma irradiation and their subsequent enzymatic hydrolysis. By investigating a range of irradiation doses (0–300 kGy), it was demonstrated how irradiation-induced molecular modifications, such as chain scission, and cross-linking, influencing the polymers thermal and mechanical properties and susceptibility to enzymatic hydrolysis. At moderate irradiation levels (25–50 kGy), which are commonly used for sterilization of medical packaging [47] PBF films exhibited enhanced enzymatic degradation. This improvement is likely due to disruption of the amorphous regions, which facilitate enzyme access and catalytic activity [48]. The release of monomeric hydrolysis products, such as 2, 5-furandicarboxylic acid and 1,4-butanediol at these doses confirms the increased susceptibility of irradiated PBF films to enzymatic hydrolysis, which indicates improved biodegradability as previously shown for other polyesters [24]. At higher irradiation doses (100–300 kGy) the polymer degradation mechanism is more complex. While the weight loss during hydrolysis increased, monomer release did not proportionally, suggesting formation of radiation-induced crosslinking. These results are consistent with prior studies on radiation-induced degradation in polyesters, where high doses promote both scission and crosslinking [49]. Thermal analyses supported these findings: glass transition temperature (T_g) and melting enthalpies decreased with dose, indicating chain scission. However, the decrease in melt crystallization temperatures and changes in thermal degradation profiles at higher doses suggest possible cross-linking/branching and reduced chain mobility, aligning with the observed tendency for mechanical behavior and decrease in susceptibility to enzymatic hydrolysis. These findings underscore the dual role of gamma irradiation as both, a sterilization and functional modification tool. When optimized, irradiation can increase the biodegradability of PBF without compromising its performance, supporting sustainable medical packaging solutions that meet hygiene requirements and facilitate end-of-life biodegradation. This dual functionality approach aligns with circular economy goals, particularly for bio-based polymers like PBF that already offer a lower environmental impact compared to its petrochemical counterparts [50].

CRediT authorship contribution statement

Maddalena Negrin: Data curation, Investigation. **Ignacio Solaberrieta:** Data curation, Investigation, Visualization, Writing – original draft. **Andrea Soldini:** Data curation, Investigation, Writing – original draft. **Mario Mariani:** Data curation, Investigation, Writing – original draft. **Elena Macerata:** Data curation, Investigation, Writing – original draft. **Patrizia Cinelli:** Data curation, Investigation. **Felice Quartinello:** Supervision, Writing – review & editing. **Sara Filippi:** Data curation, Investigation. **Bettina Semler:** Data curation, Investigation, Validation, Visualization, Writing – original draft. **Debora Puglia:** Funding acquisition, Project administration, Resources, Writing – review & editing. **María Carmen Garrigós:** Data curation, Investigation. **Guebitz Georg:** Conceptualization, Methodology, Resources, Writing – review & editing. **Nadia Lotti:** Conceptualization, Methodology, Supervision. **Michelina Soccio:** Writing – review & editing. **Alfonso Jiménez:** Supervision, Writing – review & editing. **Alessandro Coatti:** Data curation, Investigation, Writing – original draft.

Declaration of Competing Interest

The authors declare the following financial interests/personal relationships which may be considered as potential competing interests: Bettina Semler reports financial support was provided by University of Natural Resources and Life Sciences Vienna.

Acknowledgements

The FURIOUS project is supported by the Circular Bio-based Europe Joint Undertaking and its members. Funded by the European Union. The work described in this publication was subsidized by Horizon Europe (HORIZON) framework by the Grant Agreement Number 101112541. Views and opinions expressed are however those of the author(s) only and do not necessarily reflect those of the European Union or CBE JU. Neither the European Union nor the CBE JU can be held responsible for them. GA number for metadata: 101112541.

The authors would also like to show their appreciation to the doctoral school Advanced Biorefineries: Chemistry and Materials (ABC&M), BOKU University, Vienna, Austria.

Appendix A. Supporting information

Supplementary data associated with this article can be found in the online version at doi:10.1016/j.mtcomm.2026.114704.

Data availability

Data will be made available on request.

References

[1] Y.H.V. Soong, M.J. Sobkowicz, D. Xie, Recent advances in biological recycling of polyethylene terephthalate (PET) plastic wastes, *2022, Vol 9, Page 98*, Bioengineering 9 (2022) 98.
[2] K. Loos, R. Zhang, I. Pereira, B. Agostinho, H. Hu, D. Maniar, N. Sbirrazzuoli, A.J. D. Silvestre, N. Guigo, A.F. Sousa, A perspective on PEF synthesis, properties, and end-life, Front Chem. 8 (2020) 542806.
[3] S. Weinberger, J. Canadell, F. Quartinello, B. Yeniad, A. Arias, A. Pellis, G. M. Guebitz, Enzymatic degradation of poly(ethylene 2,5-furanoate) powders and amorphous films, *2017, Vol 7, Page 318*, Catalysts 7 (2017) 318.
[4] L. Maini, M. Gigli, M. Gazzano, N. Lotti, D.N. Bikiaris, G.Z. Papageorgiou, Structural investigation of poly(ethylene furanoate) polymorphs, *2018, Vol 10, Page 296*, Polymers 10 (2018) 296.
[5] A.M. Ahmed, T.P. Kainulainen, J.A. Sirviö, J.P. Heiskanen, Renewable furfural-based polyesters bearing sulfur-bridged difuran moieties with high oxygen barrier properties, Biomacromolecules 23 (2022) 1803–1811.
[6] L. Sun, J. Wang, S. Mahmud, Y. Jiang, J. Zhu, X. Liu, New insight into the mechanism for the excellent gas properties of poly(ethylene 2,5-furandicarboxylate) (PEF): role of furan ring's polarity, Eur. Polym. J. 118 (2019) 642–650.
[7] X. Fei, J. Wang, X. Zhang, Z. Jia, Y. Jiang, X. Liu, Recent progress on bio-based polyesters derived from 2,5-furandicarbonxylic acid (FDCA), Polym. (Basel) 14 (2022) 625.
[8] P. Stegmann, T. Gerritse, L. Shen, M. Londo, Á. Puente, M. Junginger, The global warming potential and the material utility of PET and bio-based PEF bottles over multiple recycling trips, J. Clean. Prod. 395 (2023) 136426.
[9] A.T. Naikwadi, B.K. Sharma, K.D. Bhatt, P.A. Mahanwar, Gamma radiation processed polymeric materials for high performance applications: a review, Front Chem. 10 (2022) 837111.
[10] M. Haji-Saeid, M.H.O. Sampa, A.G. Chmielewski, Radiation treatment for sterilization of packaging materials, Radiat. Phys. Chem. 76 (2007) 1535–1541.
[11] Karina K.M. Napolitano, C.M. Borrely, SI: gamma radiation effects in packaging for sterilization of health products and their constituents paper and plastic film, Radiat. Phys. Chem. 142 (2018) 23–28.
[12] A.M. de Azevedo, P.H.P.M. da Silveira, T.J. Lopes, O.L.B. da Costa, S.N. Monteiro, V.F. Veiga-Júnior, P.C.R. Silveira, D.D. Cardoso, A.B.H. da S. Figueiredo, Ionizing radiation and its effects on thermoplastic polymers: an overview, *2025, Vol 17, Page 1110*, Polymers 17 (2025) 1110.
[13] E. Bianchi, M. Soccio, V. Siracusa, M. Gazzano, S. Thiyagarajan, N. Lotti, Poly (butylene 2,4-furanoate), an added member to the class of smart furan-based

polyesters for sustainable packaging: structural isomerism as a key to tune the final properties, ACS Sustain Chem. Eng. 9 (2021) 11937–11949.
[14] Y. Zhao, B. Zhu, Y. Wang, C. Liu, C. Shen, Effect of different sterilization methods on the properties of commercial biodegradable polyesters for single-use, disposable medical devices, Materials Science Engineering C 105 (2019) 110041.
[15] Y. Zhao, Q. Li, B. Wang, Y. Wang, C. Liu, C. Shen, Effect of electron beam irradiation dose on the properties of commercial biodegradable poly(lactic acid), poly(butylenes adipate-co-terephthalate) and their blends, Nucl. Instrum. Methods Phys. Res B 478 (2020) 131–136.
[16] M. Negrin, E. Macerata, G. Consolati, L. Di Landro, M. Mariani, Ionizing radiation effects on polymer biodegradation, Radiat. Eff. Defects Solids 173 (2018) 842–850.
[17] Č. Novotný, K. Malachová, G. Adamus, M. Kwiecień, N. Lotti, M. Soccio, V. Verney, F. Fava, Deterioration of irradiation/high-temperature pretreated, linear low-density polyethylene (LLDPE) by Bacillus amyloliquefaciens, Int Biodeterior. Biodegrad. 132 (2018) 259–267.
[18] S. Weinberger, J. Canadell, F. Quartinello, B. Yeniad, A. Arias, A. Pellis, G. M. Guebitz, Enzymatic degradation of poly(Ethylene 2,5-furanoate) powders and amorphous films, Catalysts 7 (2017).
[19] S. Weinberger, K. Haernvall, D. Scaini, G. Ghazaryan, M.T. Zumstein, M. Sander, A. Pellis, G.M. Guebitz, Enzymatic surface hydrolysis of poly(ethylene furanoate) thin films of various crystallinities, Green. Chem. 19 (2017) 5381.
[20] K. Haernvall, S. Zitzenbacher, H. Amer, M.T. Zumstein, M. Sander, K. McNeill, M. Yamamoto, M.B. Schick, D. Ribitsch, G.M. Guebitz, Polyol structure influences enzymatic hydrolysis of bio-based 2,5-furandicarboxylic acid (FDCA) polyesters, Biotechnol. J. 12 (2017).
[21] C. Siracusa, F. Quartinello, M. Soccio, M. Manfroni, N. Lotti, A. Dorigato, G. M. Guebitz, A. Pellis, On the selective enzymatic recycling of poly(pentamethylene 2,5-furanoate)/poly(lactic acid) blends and multiblock copolymers, ACS Sustain Chem. Eng. 11 (2023).
[22] G. Dargó, D. Kis, A. Ráduly, V. Farkas, J. Kupai, Furandicarboxylic Acid (FDCA): electrosynthesis and its facile recovery from polyethylene furanoate (PEF) via depolymerization, ChemSusChem 18 (2025) e202401190.
[23] M. Sokołowska, M. Zarei, M.El Fray, Enzymatic synthesis of furan-based copolymers: material characterization and potential for biomedical applications, Polim. Med 54 (2024) 59–69.
[24] K. Haernvall, S. Zitzenbacher, K. Wallig, M. Yamamoto, M.B. Schick, D. Ribitsch, G. M. Guebitz, Hydrolysis of ionic phthalic acid based polyesters by wastewater microorganisms and their enzymes, Environ. Sci. Technol. 51 (2017).
[25] M. Nagl, R. Peters, N. Schwaiger, M. Horvat-Kocová, G.M. Guebitz, Correlation of enzymatic hydrolysis and biodegradation of coated cellulose sheets, Ind. Biotechnol. 20 (2024) 225–235.
[26] E. Bianchi, M. Soccio, V. Siracusa, M. Gazzano, S. Thiyagarajan, N. Lotti, Poly (alkylene 2,4-furanoate)s: the potential of structural isomerism for outstanding sustainable food packaging and unexpected evidence of self-healing microstructure, React. Funct. Polym. 203 (2024) 106010.
[27] S. Paszkiewicz, I. Irska, A. Zubkiewicz, K. Walkowiak, Z. Rozwadowski, J. Dryzek, A. Linares, A. Nogales, T.A. Ezquerra, Supramolecular structure, relaxation behavior and free volume of bio-based poly(butylene 2,5-furandicarboxylate)-block-poly(caprolactone) copolyesters, Soft Matter 19 (2023).
[28] Y. Wang, K. Su, C. Liu, Z. Li, Poly(butylene 2,5-furandicarboxylate) copolyester obtained using 1,6-hexanediamine with high glass transition temperature, RSC Adv. 13 (2023).
[29] S. Mahmud, Y. Long, M. Abu Taher, H. Hu, R. Zhang, J. Zhu, Fully bio-based micro-cellulose incorporated poly(butylene 2,5-furandicarboxylate) transparent composites: preparation and characterization, Fibers Polym. 21 (2020).
[30] N. Bansal, S. Arora, Exploring the impact of gamma rays and electron beam irradiation on physico-mechanical properties of polymers & polymer composites: a comprehensive review, Nucl. Instrum. Methods Phys. Res B (2024) **549**.
[31] C. Ferrante, L. Lucchesi, A. Cemmi, I. Di Sarcina, J. Scifo, A. Verna, A. Taschin, L. Senni, M. Beghini, B.D. Monelli, et al., Gamma irradiation effect on polymeric chains of epoxy adhesive, *2024, Vol 16, Page 1202*, Polymers 16 (2024) 1202.
[32] A.T. Naikwadi, B.K. Sharma, K.D. Bhatt, P.A. Mahanwar, Gamma radiation processed polymeric materials for high performance applications: a review, Front Chem. 10 (2022) 837111.
[33] C. Vasile, D. Pamfil, T. Zaharescu, R.P. Dumitriu, G.M. Pricope, M. Râpă, G. Vasilievici, Effect of gamma irradiation on the pla-based blends and biocomposites containing rosemary ethanolic extract and chitosan, Polym. (Basel) 14 (2022).
[34] J.C.M. Suarez, E.E. Da Costa Monteiro, E.B. Mano, Study of the effect of gamma irradiation on polyolefins-low-density polyethylene, Polym. Degrad. Stab. 75 (2002).
[35] M. Kattan, Thermal behavior of gamma-irradiated amorphous poly (ethylene terephthalate) films, Polym. Eng. Sci. 46 (2006).
[36] M. Sirin, M.S. Zeybek, K. Sirin, Y. Abali, Effect of gamma irradiation on the thermal and mechanical behaviour of polypropylene and polyethylene blends, Radiat. Phys. Chem. 194 (2022).
[37] B. Kurbanova, K. Aimaganbetov, K. Ospanov, K. Abdrakhmanov, N. Zhakiyev, B. Rakhadilov, Z. Sagdoldina, N. Almas, Effects of electron beam irradiation on mechanical and tribological properties of PEEK, Polym. (Basel) 15 (2023) 1340.
[38] M.S. Iorshase, A. Abubakar Sadiq, L.J. Utume, E.O. Adamu, M. Sani, W.S. Oyeyemi, Impacts of high-dose gamma irradiation on the mechanical, structural and thermal properties of doum fiber reinforced high-density polyethylene (HDPe), Recent Adv. Nat. Sci. (2025), https://doi.org/10.61298/RANS.2025.3.1.200.
[39] A.T. Naikwadi, B.K. Sharma, K.D. Bhatt, P.A. Mahanwar, Gamma radiation processed polymeric materials for high performance applications: a review, Front Chem. 10 (2022) 837111.
[40] M.M. Nasef, O. Güven, Radiation-grafted copolymers for separation and purification purposes: status, challenges and future directions, Prog. Polym. Sci. 37 (2012).
[41] L.F. de Miranda, L.H. Silveira, L.G. Andrade e Silva, A.H. Munhoz Jr., Irradiation of a polypropilene-glass fiber composite, 12th Int. Ceram. Congr. PART J. (2010).
[42] M.M. Nasef, B. Gupta, K. Shameli, C. Verma, R.R. Ali, T.M. Ting, Engineered bioactive polymeric surfaces by radiation induced graft copolymerization: strategies and applications, Polym. (Basel) 13 (2021).
[43] A. Eberl, S. Heumann, T. Brückner, R. Araujo, A. Cavaco-Paulo, F. Kaufmann, W. Kroutil, G.M. Guebitz, Enzymatic surface hydrolysis of poly(ethylene terephthalate) and bis(benzoyloxyethyl) terephthalate by lipase and cutinase in the presence of surface active molecules, J. Biotechnol. 143 (2009).
[44] S. Kaabel, Daniel Therien, J.P. Deschênes, C.E. Duncan, D. Friščic, T. Auclair, K: Enzymatic depolymerization of highly crystalline polyethylene terephthalate enabled in moist-solid reaction mixtures, Proc. Natl. Acad. Sci. USA 118 (2021) e2026452118.
[45] Di Bisceglie F., Quartinello F., Vielnascher R., Guebitz G.M., Pellis A.: Cutinase-Catalyzed Polyester-Polyurethane Degradation: Elucidation of the Hydrolysis Mechanism. 2022, doi:10.3390/polym14030411.
[46] R. Brackmann, C. de Oliveira Veloso, A.M. de Castro, M.A.P. Langone, Enzymatic post-consumer poly(ethylene terephthalate) (PET) depolymerization using commercial enzymes, 3 Biotech 13 (2023) 135.
[47] T. Sandle, Application of sterilization by gamma radiation for single-use disposable technologies in the biopharmaceutical sector, J. GXP Compliance (2012).
[48] R. Wei, W. Zimmermann, Microbial enzymes for the recycling of recalcitrant petroleum-based plastics: how far are we? Micro Biotechnol. 10 (2017) 1308–1322.
[49] K. Makuuchi, S. Cheng, Radiation processing of polymer materials and its industrial applications, Radiat. Process. Polym. Mater. Ind. Appl. (2011), https://doi.org/10.1002/9781118162798.
[50] A.M. de Azevedo, P.H.P.M. da Silveira, T.J. Lopes, O.L.B. da Costa, S.N. Monteiro, V.F. Veiga-Júnior, P.C.R. Silveira, D.D. Cardoso, A.B.H. da S. Figueiredo, Ionizing radiation and its effects on thermoplastic polymers: an overview, *2025, Vol 17, Page 1110*, Polymers 17 (2025) 1110.